

# NOISE REDUCTION IN THREE PHASE VOLTAGE SOURCE INVERTER FED IM USING RANDOM SVPWM TECHNIQUE

**R.Mohandas**

Assistant Professor, Sri Shakthi institute of Engineering and Technology, Coimbatore.

**E.Chandirasekaran**

Associate Professor, Coimbatore Institute of Technology, Coimbatore

**Abstract** – *The paper focus to study on noise reduction of the line voltage of two level three phase voltage source inverter (VSI) fed induction motor (IM) at the specific frequency, and developed new PWM called Random Space Vector Pulse width modulation technique (RSVPWM) for reducing noise on line voltage. The developed RSVPWM is combining RPWM and Space vector modulation (SVPWM) technique. The paper also investigates the three-phase VSI fed induction motor and its noise behavior. The proposed method is able to create a gap in the spectrum of line voltage at selective frequency in human hearing range. Therefore, unlike conventional RPWM techniques, switching periods are determined based on the position of rotary reference vector. The paper compared with other PWM such as SPWM, RPWM and SVPWM. Among all PWM method the proposed RSVPWM generate higher voltages with low total harmonic distortion. The proposed RSVPWM is receipt less line voltage noise (10.4dB at lower modulation range and 9dB at higher modulation range). The simulation and experimentation is carried out for the full range of switching frequency of 1 kHz to 20 kHz. The modulation method can be used in both open- and closed-loop IM drive such as V/F and vector control.*

**Keywords:** *Random Space Vector Pulse width modulation, Acoustic noise, Power spectral density, three phase voltage source inverters, resonant frequency excitation.*

## 1. Introduction

Most of the industrial drives produce heavy noise in the environment. The friction, imbalance, and aerodynamic origin cause acoustic noise, especially at low speed. The human ear is the usual receiver for noise. The Human ear responds for sounds varies over a frequency range from about 16-20 Hz up to frequencies in the 16-20 kHz range [1]. Many papers recommend RPWM method to avoid whistling and EMI noise in three phase VSI. The various randomization techniques are implemented by the converter fed drive system [2]. The first order sigma modulator used for the SVPWM technique to

spread the harmonics for the desired range [3]. The author [4] suggests the quasi- random modulation strategy used for the Acoustic Noise in the VSI. The emitted acoustic noise is reduced using randomly varying switching frequency within the pre specified bands. The modulation in the random scheme determines the mechanical resonances and wide range of frequency of the voltage spectrum can be spread [5].

Random modulation technique is used for adjusting the duration of the zero vectors or adjusting the three pulse positions in a switching period with fixed switching frequency. The mitigation of electromagnetic interference and acoustic noise in vehicular drives by fixed and random PWM technique [6, 7, 21-24]. In inverter fed drive system using digital modulator, a constant switching period is equal to the sampling period for mitigation of noise in the system. The switching periods and random PWM method with a constant sampling period are randomly varied. The sampling period equal to the randomly varied switching period around an average value [8]. The basic motor control algorithm has minimal impact on variable delay random PWM technique. Even with asynchronous current sampling, the current regulation is found optimal. In the low-speed motor this technique deployed to reduce switching losses of the inverter [9]. Three types of randomized pulse position modulation techniques are proposed in indirect matrix converter. Those techniques are carrier based randomize the pulse position modulation of an indirect matrix converter [10]. A two-dimensional random switching pulse width modulation schemes diminishes the harmonic clusters while simultaneously retaining constant average inductor current and constant sampling frequency. The output voltage ripple is reduced by constant average inductor current [11]. Pederson *et al.*, reduced noise power in specified interval in frequency domain by

removing determined range or ranges from switching frequencies. Along with providing a gap in the frequency spectrum, this method leads to increase in peak of Power Spectrum Density (PSD) diagram. In Electric drive System without Exciting Mechanical Resonance, A new fixed carrier frequency quasi- random PWM method to generate acoustical noise by the drive can be improved [12]. Randomly centered distribution (RCD) problem is solved by the two-phase dual zero vector random centered distribution scheme. Modulation index of RCD is high and not reduced properly [13]. Fixed and randomized PWM technique for the fully controlled converter reduces the harmonic intensity for contributing the efficiency [14, 15]. The asymmetric carrier wave to implement digitally, without employing external circuit [16, 17]. Sinusoidal PWM and SVPWM utilize a changing carrier frequency to spread the harmonics in a wideband area thereby achieving great reduction in harmonics. The SVPWM gives 15% improved fundamental output with better quality [18]. New RSPWM technique used to provide gap in the spectrum of line voltage to prevent the system resonant frequency excitation [19].

In this paper, a RSPWM technique is employed to reduce noise from the line voltage of two level three phase voltage source inverter. The proposed method can prevent the excitation of system resonant frequency. The remaining paper been organized as noise investigation in random and SVPWM technique, review of random space vector pulse width modulation, simulation and experimental results and conclusion of proposed system.

### 3. Review of Three-Phase VSI Fed Induction Motor and Its Noise Behavior

The Fig.1 shows the three-phase six switch VSI fed induction motor. The three-phase voltage source inverter consist of six semiconductor switches ( $S_1$  to  $S_6$ ) and they are conducting in 180-degree phase shift between their upper and lower switches. There are six intervals of operation in VSI which are 60 degree each. In every interval either one upper and two lowers, or two upper and one lower switches are tuned on for symmetry operation of the inverter. Totally eight possible combinations of on and off process for the three phase VSI, which are represented from the switching position of upper lag

or in lower leg. In this paper following upper switching positions. Example, in mode-1 all upper switches are “OFF”. Hence the switching representation of this state is used as [000], like in mode-2, phase A leg and phase B leg upper switch are ‘ON’, and phase C lower switch is ‘OFF’ (phase C lower switch is ‘ON’). Hence the switching representation of this state is used as [110]. The table 1 illustrate all mode of operation switching and its corresponding line and phase voltages. Form the eight possible combinations six is called as active inverter modes and other two ([111], [000]) zero vector modes. In active mode, the dc-link voltage is connected to load, where as in [111] and [000] mode dc-link and load is isolated.

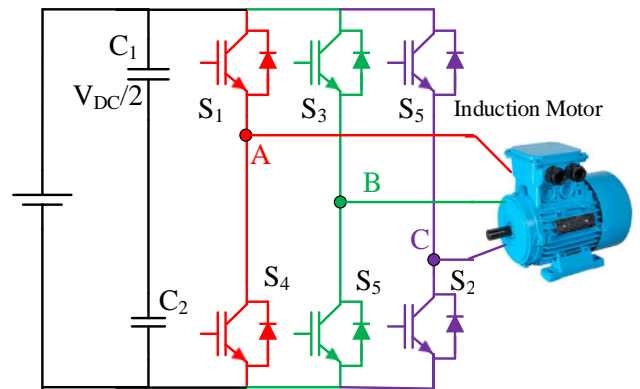


Fig.1. Three Phase Inverter fed Induction Motor

To control the power switches from the inverter, numerous modulation approaches were reported in literature [20]. In which sine PWM (SPWM) and space vector PWM (SVPWM) are the frequently used one and all modified PWM techniques are developed from SPWM and SVPWM. The SVPWM and its switching is explained though Fig.2. In SVPWM is reference vector  $V^*$  is sampled with a frequency  $f_s$  ( $T_s = 1/f_s$ ). The  $V^*$  generated from three-phase 120-degree phase shift references using the alpha -beta transformation. The space vector diagram (SVD) is consist of six-sector and each sector is synthesized using three adjacent switching states (vectors). The  $V^*$  is synthesized using a two adjacent active switching vectors and one zero vector (either [111] / [000]). By using zero vector pation in forming vector sequence the SVPWM can be modified as continuous and discontinuous SVPWM. The strategy selection will have focused for reducing harmonic content and the switching

losses. Fig.3 shows the sector-1 switching states and its pulse pattern.

Table 1. VSI switching vector, phase voltage and line voltage.

Mode	Voltage Vector	Switching vector			Line to Line voltage		
		A	B	C	V <sub>ab</sub>	V <sub>bc</sub>	V <sub>ca</sub>
1	V <sub>0</sub>	0	0	0	0	0	0
2	V <sub>1</sub>	1	0	0	1	0	0
3	V <sub>2</sub>	1	1	0	0	1	-1
4	V <sub>3</sub>	0	1	0	-1	1	0
5	V <sub>4</sub>	0	1	1	-1	0	1
6	V <sub>5</sub>	0	0	1	0	-1	1
7	V <sub>6</sub>	1	0	1	1	-1	0
8	V <sub>7</sub>	1	1	1	0	0	0

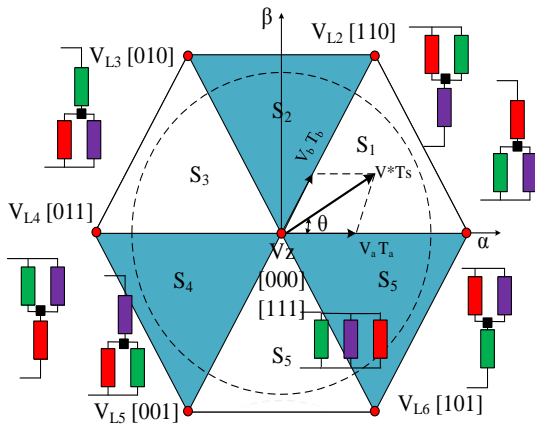


Fig.2. Space vector diagram (SVD) and switching

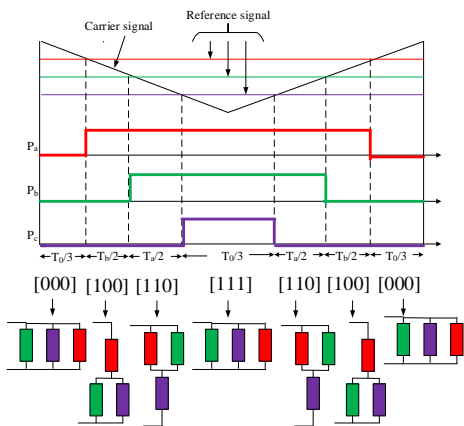


Fig.3. sector-1 switching scheme

The switching Pattern for each sector in SVD is shown in Fig 4.

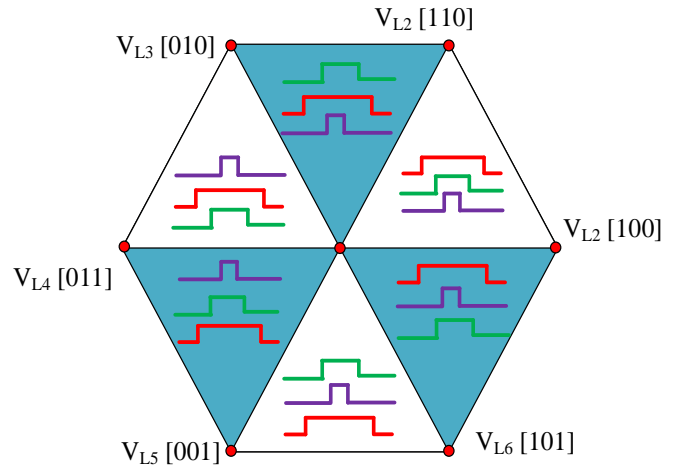


Fig.4. Switching pattern for each sector of SVD

Here the reference is generated by using on-time equations of the SVD. Then the symmetrical carrier is compared with reference signal. The SPWM and SVPWM is similar way of approach. In SPWM, the three-phase reference signal directly compared with carrier signal, where as in SVPWM composed time manner and finally compared with carrier signal. Though SPWM and SVPWM is a frequently used method for all VSI applications. These methods had a discrete frequency components in their current spectrum which cause the EMI and acoustic noise in the induction motor. To distribute the discrete components from the current spectrum of the motor is called as RPWM. There are few concepts were developed in RPWM approaches which can reduces the EMI and lower order harmonics.

### 3. Noise Investigation

When the induction motor is operated in non-sinusoidal power supply (quasi-square wave form) the acoustic noise is created on the starter. This may excite the system resonant frequencies which increases the acoustic noise and vibration [13-15]. For acoustic noise reduction, a weighted IEC 61672-2013-standard range of RPWM method compared to conventional RPWM technique is to reduce broad band noise by 2-6 dB over the full modulation index range. This range produces a better acoustic noise. Acoustic noise generated by electrical motors driven

by a pulse width modulated power electronic inverter. Various PWM techniques (i.e. SPWM, RPWM, FCF-RPWM, RCF-RPWM, and SVPWM) are used to reduce the greatest annoyance of the motor. The proposed method of RSVPWM technique used to reduce the acoustic noise below 10 dB. The human ear is the remarkable acoustic system. The ear is capable of responding to sounds over a frequency range from about 16-20Hz up to frequencies in the 16-20 kHz range. Above 20 kHz is the greatest annoyance. The acoustic noise creates an unpleasant atmosphere to work and the mechanical vibration causes gap separation between the stator and rotor. The best way to reduce audible noise radiated from the AC motor is to increase the PWM switching frequency up to 18 kHz. A randomized pulse position method in which, the discrete harmonics are significantly reduced and harmonic power spread over as a continuous spectrum. The discrete harmonic spectra occur at switching frequency and its multiples. The normal voltage source inverter produces the noise shown in Fig. 5, it was analyzed by spectrum scope. The acoustic noise produced above 20 dB for the three-phase voltage source PWM inverter. Fig. 6 shows the spectrum of noise in three phase VSI.

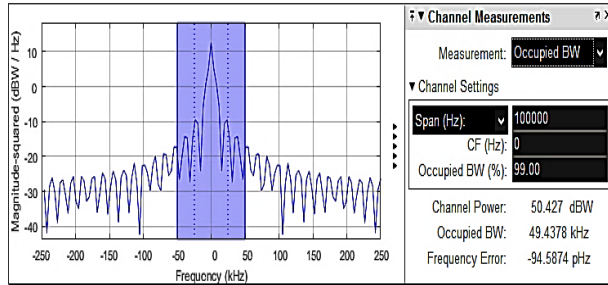


Fig.5. Spectrum of VSI line voltage

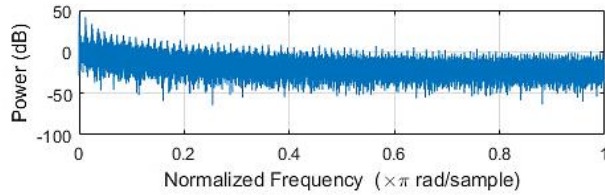


Fig.6. Noise power dB

### 3. Proposed Random SVPWM Technique

As mentioned in the section-2 the SVPWM has several advantages over the SPWM such as: low common mode current and switching loss. In this section, the capability of SVPWM and RPWM for noise reduction has been evaluated when the switching frequency is selected randomly. In this way, first in each cycle the switching

period is selected from the proper range, then according to time percentage of  $d_a$ ,  $d_b$ , and  $d_o$ , the switching pulses has been generated.

From the SVPWM generation block random carrier is created and PWM pulses are generated. The basic diagram of RPWM is shown in Fig.7 and the flow chart for producing RSVPWM is shown in Fig 8.

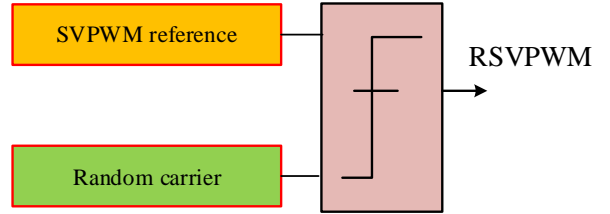


Fig.7. RSVPWM signal generator

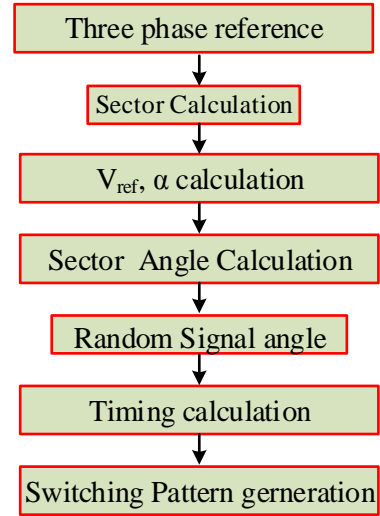


Fig.8 Flow Chart for Producing RSPWM

Initially the three-phase reference is generated and they are sampling in to  $V_d$  and  $V_q$ . The magnitude (reference voltage vector,  $V^*$ ) and angle ( $\alpha$ ) of  $V_d$ ,  $V_q$  is calculated from Real-Image to complex block. The  $V^*$  and  $\alpha$  is helping to find out the SVD sector and switching states.

$$\begin{aligned} V_d &= V_{an} - V_{bn} \cos 60^\circ - V_{cn} \cos 60^\circ \\ &= V_{an} - \frac{1}{2}V_{bn} - \frac{1}{2}V_{cn} \end{aligned} \quad (1)$$

$$\begin{aligned} V_q &= 0 + V_{bn} \cos 30^\circ - V_{cn} \cos 30^\circ \\ &= 0V_{an} + \frac{\sqrt{3}}{2}V_{bn} - \frac{\sqrt{3}}{2}V_{cn} \end{aligned} \quad (2)$$

$$\begin{bmatrix} V_d \\ V_q \end{bmatrix} = \frac{2V_s}{3} \begin{bmatrix} 1 & -1/2 & -1/2 \\ 0 & \sqrt{3}/2 & -\sqrt{3}/2 \end{bmatrix} \begin{bmatrix} V_{an} \\ V_{bn} \\ V_{cn} \end{bmatrix}$$

$$|V_{ref}| = \sqrt{V_d^2 + V_q^2} \quad (3)$$

$$\alpha = \tan^{-1}\left(\frac{V_q}{V_d}\right) = \omega t = 2\pi f t \quad (4)$$

In order to create the random pulses in the SVPWM pulses, the random carrier is created and sampled with  $V^*$  and  $\alpha$ . Fig.9 shows the random carrier signal of 5 kHz. There are 10 timing is fixed (0 1.5/fs 3/fs 4.5/fs 6/fs 7/fs 8/fs 9/fs 10/fs) to creating the Fig.9 carrier signal.

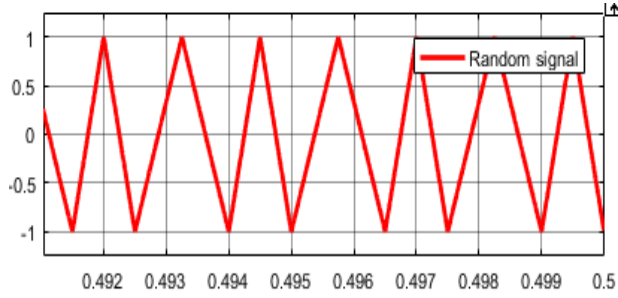


Fig.9 Random carrier signal

Next the angle  $\gamma$  is calculated with in the sector. The maximum values  $\gamma$  is 60 degree which to find out the exact location of the  $V^*$ . The timing calculation of the switching vector is calculated by using eq (5) to (9)

$$\int_0^{T_0} V_{ref} dt = \int_0^{T_1} V_1 dt + \int_{T_1}^{T_1+T_2} V_2 dt + \int_{T_1+T_2}^{T_0} V_0 dt \quad (5)$$

$$V_{ref} [T_0] = V_1 [T_1] + V_2 [T_2] + V_0 [T_0 - T_1 - T_2] \quad (6)$$

$$V_{ref} T_0 \begin{bmatrix} \cos \alpha \\ \sin \alpha \end{bmatrix} = \frac{2V_s}{3} T_1 \begin{bmatrix} \cos 0 \\ \sin 0 \end{bmatrix} + \frac{2V_s}{3} T_2 \begin{bmatrix} \cos \pi/3 \\ \sin \pi/3 \end{bmatrix}$$

Hence,

$$T_1 = \frac{\sqrt{3}T_s V_{ref}}{V_{dc}} \sin\left(\frac{\pi}{3} - \theta\right) \quad (7)$$

$$T_2 = \frac{\sqrt{3}T_s V_{ref}}{V_{dc}} \sin(\theta), 0 \leq \theta \leq \frac{\pi}{3} \quad (8)$$

$$T_s = T_0 - (T_1 + T_2) \quad (9)$$

Where, ( $T_s = 1/fs$ ) is a switching time,  $T_1$  and  $T_2$  is the on-time,  $T_0$  is off time (commutation time)

Once the time calculation has done, the correspondence switching states selection is chosen based on the sector number. The Fig.10 show the vector selection of RSV PWM. The switching states are mapped to get a symmetry pulse structure, which ensure the better harmonics profiles and dc-link

voltage utilization. RSV PWM train when pulses are located at the centre of switching period of SVPWM.

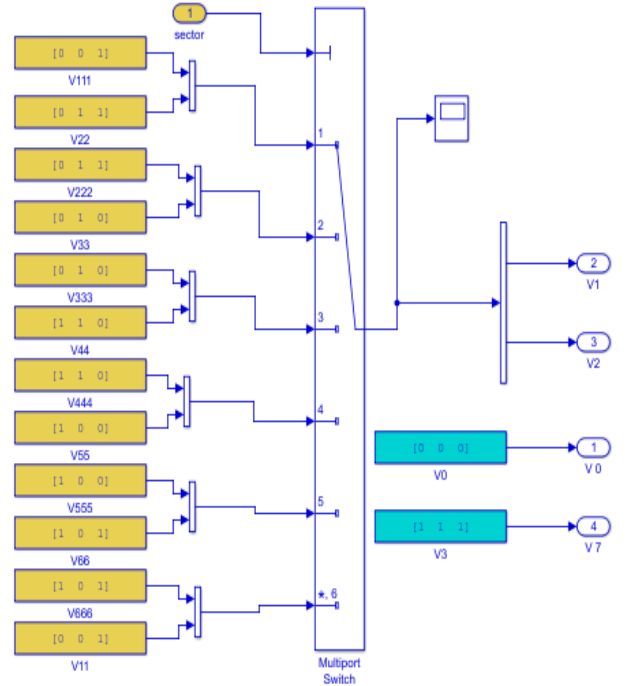


Fig.10 vector selection of RSV PWM

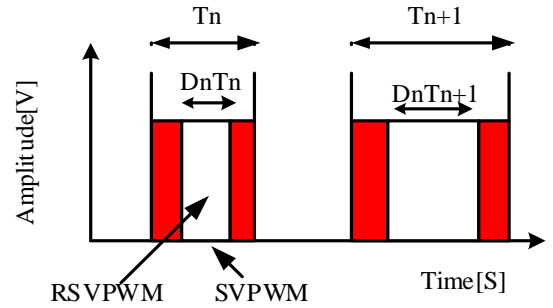


Fig.11 Pulse pattern of SVPWM and RSV PWM train when pulses are located at the centre of switching period

The switching time at each sector is summarized in Table-2. The phase voltages consist of pulse train as shown in Fig. 11. For the case in which pulses are located at the beginning of switching period, to remove noise from pulse train a formula has been derived as,

$$T_{n+1} = \frac{k}{f_o} (1 - D_n) T_1 \quad (10)$$

where  $T_n$  is switching period of nth cycle,  $D_n$  is duty ratio of nth cycle,  $k$  is a natural random number, and  $f_o$  is desired frequency for eliminating noise.

By replacing  $t_{n+1}$  with  $t_n + T_n$  in (10) the switching periods, for eliminating noise at  $f_o$  from spectrum, has been calculated as,

$$T_{n+1} = \frac{2K - (1 + D_n)f_o T_n}{(1 + D_n)f_o} \quad (11)$$

Table -2 switching time at each sector

Sector	Upper Switches ( $S_1, S_3, S_5$ )	Lower Switches ( $S_4, S_6, S_2$ )
1	$S_1 = T_1 + T_2 + T_0/2$ $S_3 = T_2 + T_0/2$ $S_5 = T_0/2$	$S_4 = T_0/2$ $S_6 = T_1 + T_0/2$ $S_2 = T_1 + T_2 + T_0/2$
2	$S_1 = T_2 + T_0/2$ $S_3 = T_1 + T_2 + T_0/2$ $S_5 = T_0/2$	$S_4 = T_2 + T_0/2$ $S_6 = T_0/2$ $S_2 = T_1 + T_2 + T_0/2$
3	$S_1 = T_0/2$ $S_3 = T_1 + T_2 + T_0/2$ $S_5 = T_2 + T_0/2$	$S_4 = T_1 + T_2 + T_0/2$ $S_6 = T_0/2$ $S_2 = T_1 + T_0/2$
4	$S_1 = T_0/2$ $S_3 = T_1 + T_0/2$ $S_5 = T_1 + T_2 + T_0/2$	$S_4 = T_1 + T_2 + T_0/2$ $S_6 = T_2 + T_0/2$ $S_2 = T_0/2$
5	$S_1 = T_2 + T_0/2$ $S_3 = T_0/2$ $S_5 = T_1 + T_2 + T_0/2$	$S_4 = T_1 + T_0/2$ $S_6 = T_1 + T_2 + T_0/2$ $S_2 = T_0/2$
6	$S_1 = T_1 + T_2 + T_0/2$ $S_3 = T_0/2$ $S_5 = T_1 + T_0/2$	$S_4 = T_0/2$ $S_6 = T_1 + T_2 + T_0/2$ $S_2 = T_2 + T_0/2$

#### 4. Simulation and Results

In order to investigate the proposed RSVPM for VSI fed induction motor noise elimination, the 0.75 kW induction motor connected six switches VSI is designed in MATLAB/Simulink platform and tested with SVPWM and proposed RSVPM for different modulation indices. The Table-3 shows the simulation parameters of the induction motor with maximum randomization freedom, the nonlinearities such as dead time and pulse filter have been ignored in the simulation. The Fig.12 shows the full simulation model for VSI fed induction motor and Fig. 13 shows the random SVPWM signal generator, where the timing calculation block is modelled by varying the carrier signal in random fashion.

Table-3 parameters of the induction motor

Power (p)	0.75 KW
Line to Line voltage ( $V_L$ )	415 V
Frequency (f)	50 Hz
Stator resistance ( $R_s$ )	1.435 $\Omega$
Stator inductance ( $L_s$ )	0.005839 H
Rotor resistance ( $R_r$ )	1.395 $\Omega$
Pole pairs (P)	2 Pole
Speed (N)	1461 rpm
Current, $I_{rms}$	3.641A
Voltage, $V_{rms}$	0.44V
Torque, T	5.865 N-m

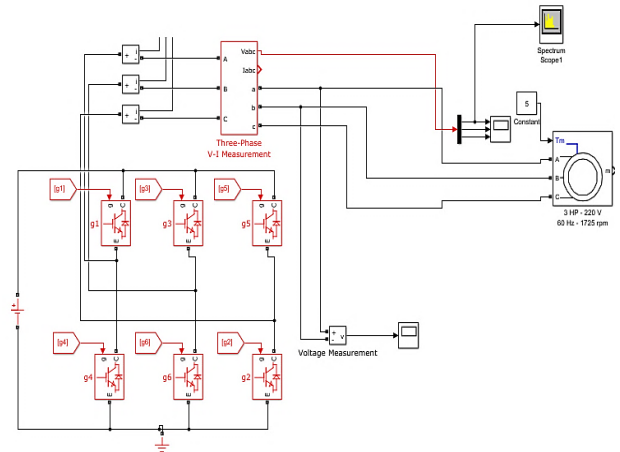


Fig.12 full simulation model for VSI fed induction motor

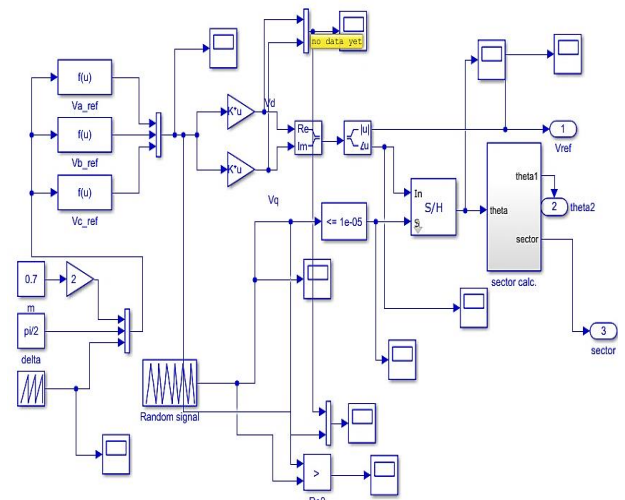


Fig. 13 random SVPWM signal generator

The inverter switching frequency is adjusted from 1 kHz to 20 kHz range and results were obtained. The Fig.14 shows the pulses ( $S_1$  to  $S_6$ ) of the inverter. Here it could see that the pulses of the inverter switches are positioned randomly. The Fig.15 shows the line voltage waveform of RSVPWM fed VSI high modulation index 0.9. When the inverter operated 0.9  $M_a$ , the line voltage is measured as 268V. Fig.16 shows the harmonics spectrum for line voltage. The percentage voltage THD is measured as 22.4% when the inverter operated in maximum operation  $M_a$  range. Fig. 16 and 17 shows the voltage noise spectrum of lower  $M_a$  (0.4) and higher  $M_a$  (0.9). When inverter operated at 0.4  $M_a$ , the noise dB is measured as 12.56. In the same switching frequency range (4 kHz), when inverter operating at 0.9  $M_a$  the noise is measured as 9dB. The lower modulation ranges the voltage waveform had more noise compared to higher modulation lines range. This is happening due to the pulse dropping. Based on the results it could understand that the proposed RSVPWM is limiting their voltage spectra noise within the recommended range.

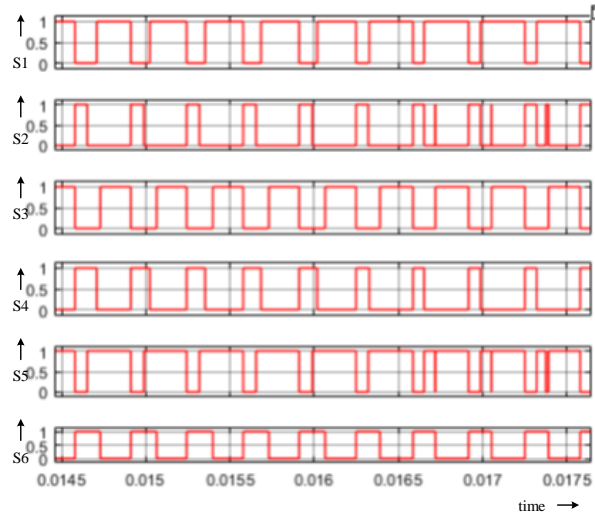


Fig. 14 random SVPWM signal generator

In order to make the comparison between SPWM, RPWM, SVPWM and RSVPWM modulation methods, the inverter simulated and the results are measured. The inverter operation condition is maintaining the same for all PWM and the results was performed for 0.5 and 0.9  $M_a$ . Fig.19 shows the simulation results of the motor voltage spectrum of modulation index 0.5 SPWM and RPWM, SVPWM, Proposed RSVPWM and Fig.20 shows the simulation

results of the motor voltage spectrum of modulation index 0.9 SPWM and RSPWM, SVPWM, proposed RSPWM.

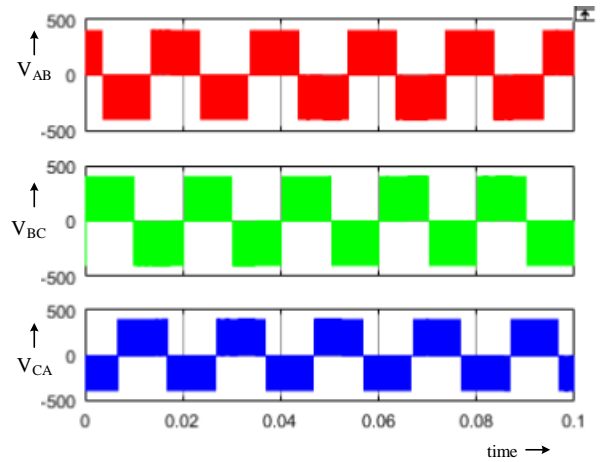


Fig. 15 RSVPWM VSI line voltage  $V_{AB}$  for  $M_a=0.9$

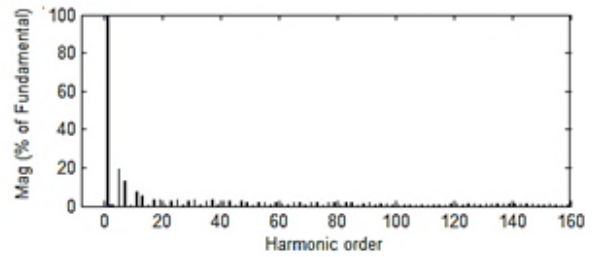


Fig. 16 Harmonics spectrum of line voltage  $V_{AB}$  for  $M_a=0.9$

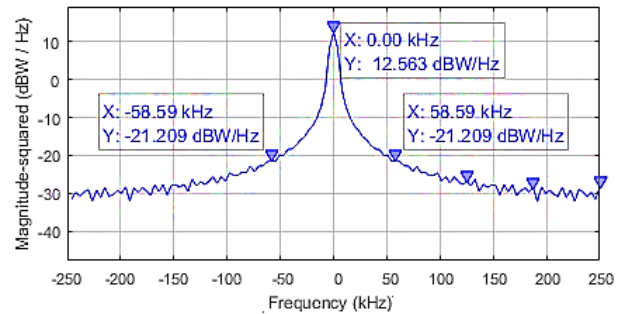


Fig. 17 RSVPWM noise spectrum for  $M_a=0.5$

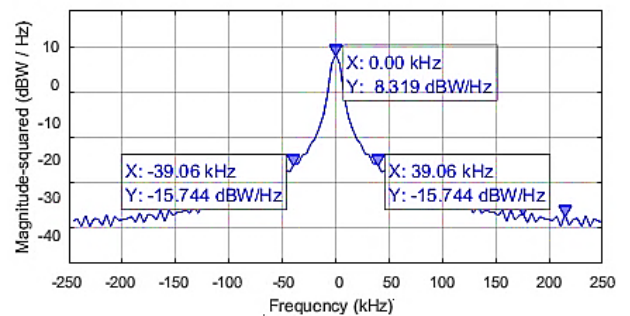


Fig. 18 RSVPWM noise spectrum for  $M_a=0.9$

From the results for both 0.5 and 0.9  $M_a$  the proposed RSPWM is has less dB compare to other reposed PWM. The RSPWM gave a similar performance, when the inverter operated wide range of switching frequency. Table-4 show the noise level for the different frequencies. Here, RPWM and RSPWM noise level is maintain the same boundary compare to other RSPWM and RPWM. Fig 21 shows the noise level in different range of frequency for all discussed PWM methods. The RSPWM is better in all the frequency range. Note; the noise is also related semiconductor switching technology. Hence, this result may differ when the different type of switches used.

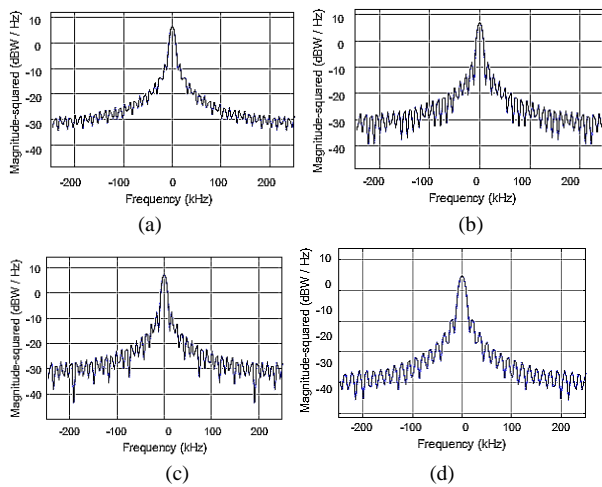


Fig. 19. Simulation results of the motor voltage spectrum for modulation index 0.5: (a) SPWM, (b) modified SPWM and (c) SVPWM (d) RSPWM

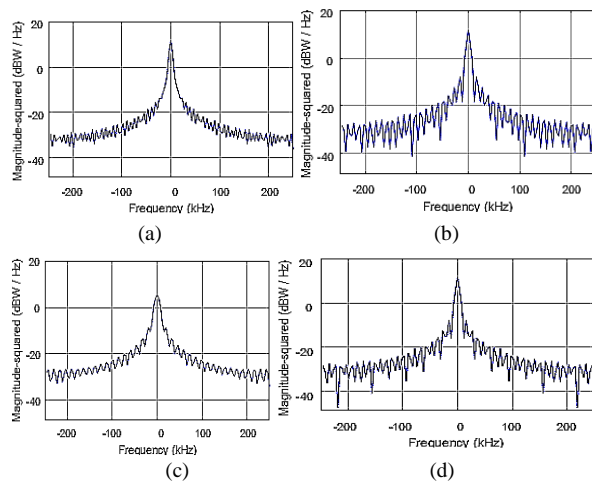


Fig. 20. Simulation results of the motor voltage spectrum for modulation index 0.8: (a) SPWM, (b) RSPWM and (c) SVPWM (d) RSPWM

Table-4 noise level for SPWM, RSPWM, SVPWM, RSPWM

$f_s$	SPWM	RSPWM	SVPWM	RSPWM
4kHz	24	14	18	9
5kHz	25	16	19.5	9
6kHz	26	17	20.4	9.2
7kHz	27	18.3	23.5	9.2
8kHz	29	18.4	20.5	9.2

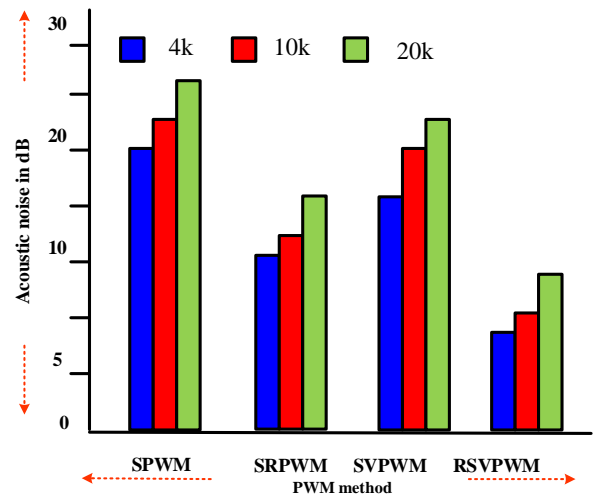


Fig.21. Switching pattern for each transistor

## 5. Experimental Results

In order to evaluate the proposed PWM performance and its acoustic noise reduction on VSI fed IM drive, the six switch 1 kW inverter power module fed 1HP (0.75kW) IM drive test bench is developed with mechanical load. Fig.22. illustrates the experimental setup of the three-phase VSI fed IM drive. In order to validate to the proposed RSPWM, the RSPWM is also preprogrammed in MATLAB/Simulink code is converted to VHDL code using Xilinx system generator tool. The developed VHDL bit file is done loaded in spartan-6 FPGA processor and the pulses are given to TLP250 gate driver circuit. The 5 volts generated pulse is given to IPM. The inverter is tested with the frequency range of 1 kHz to 15 kHz. The dead band is fixed as 5micro sec for all the range of switching frequency. The vibrations on the motor shell were measured with multianalyzer and other motor parameters are measured with fluke meter and digital oscilloscope. The was performed between 1



kHz to 15 kHz for the inverter control modulation index range from  $M_a=0.5$  to  $M_a=0.9$ . The experimentations are performed different inverter switching frequencies and the line voltage and correspond noise harmonics spectrum is recorded. Fig.23 shows the proposed RSVPWM line voltage of  $V_{AB}$  for 0.5  $M_a$  at 5 kHz and its corresponding experimental harmonics spectrum is shown in Fig.24. Similarly, for higher ( $M_a = 0.9$ ), Fig.25 shows the line voltage of  $V_{AB}$  for 0.9  $M_a$  and Fig.26 shows the Experimental harmonics spectrum of Line voltage of  $V_{AB}$  for 0.9  $M_a$ .

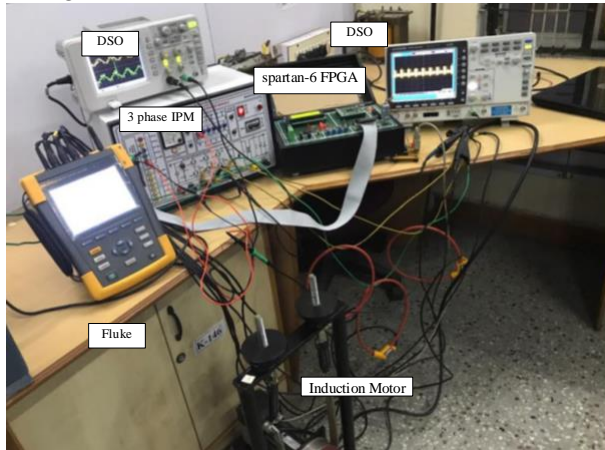


Fig.22. Experimental setup

Fig.25 shows the proposed SRPWM line voltage of  $V_{AB}$  for 0.9  $M_a$  at 5 kHz and its corresponding experimental harmonics spectrum is shown in Fig.26. Similarly, the recovered line voltage and its corresponding harmonics are tabulated and compared in Table-5. From the table, it could see that the proposed RSVPWM is has a merits of producing the higher DC-link utilization with reduced harmonics, which leads to reduce the noise in the drive.

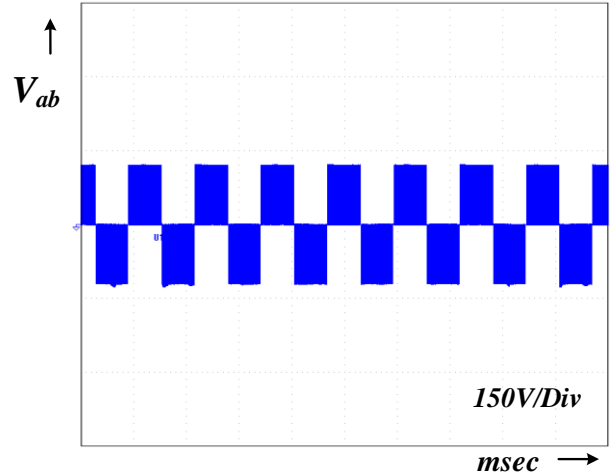


Fig.23. Experimental results of Line voltage of  $V_{AB}$  for 0.5  $M_a$

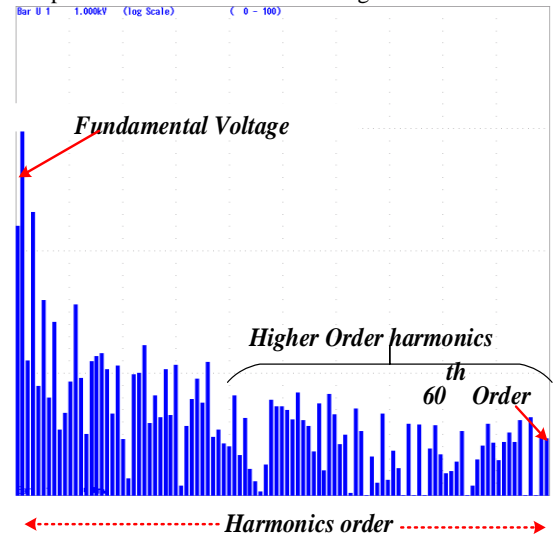


Fig.24. Experimental harmonics spectrum of Line voltage of  $V_{AB}$  for 0.5  $M_a$

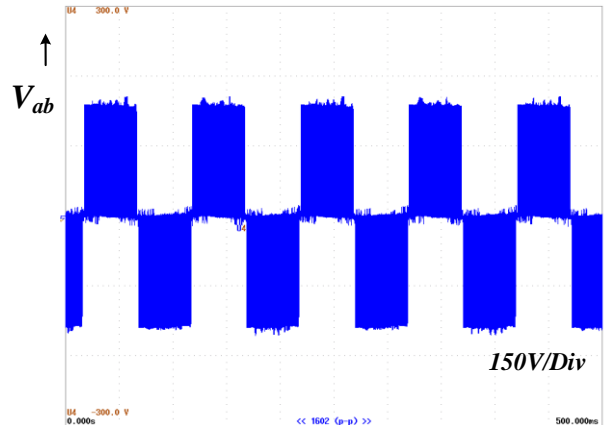


Fig.23. Experimental results of Line voltage of  $V_{AB}$  for 0.9  $M_a$

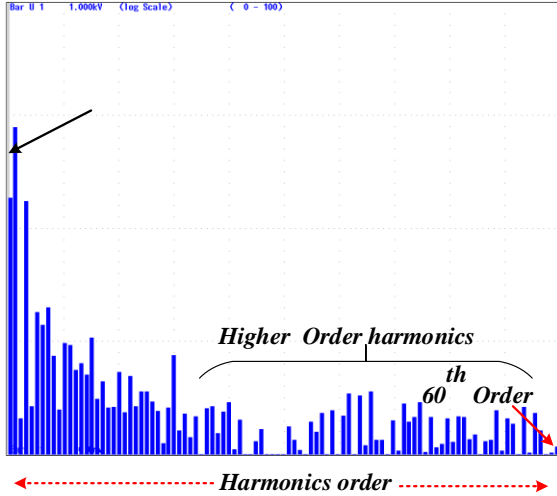


Fig.24. Experimental harmonics spectrum of Line voltage of  $V_{AB}$  for 0.9  $M_a$

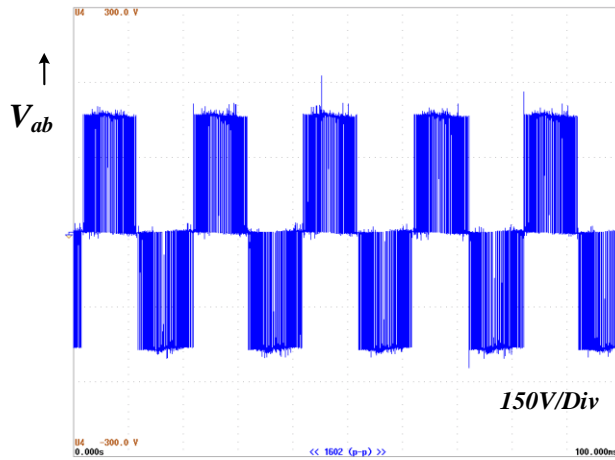


Fig.25. Experimental results of Line voltage of  $V_{AB}$  for 0.9  $M_a$

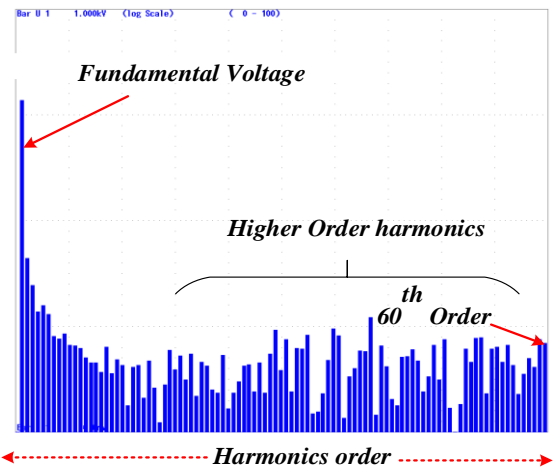


Fig.26. Experimental harmonics spectrum of Line voltage of  $V_{AB}$  for 0.9  $M_a$

Table-5 Experimental performance and comparison between RSPWM and proposed RSVPWM for 5kHz switching frequencies.

$M_a$	SPWM		MCRSPWM	
	$V_1$	% $V_{THD}$	$V_1$	% $V_{THD}$
0.1	21	42.36	23	21.2
0.2	52	43.22	54	22.359
0.3	80	41.11	85	25.990
0.4	109	44.23	113	26.10
0.5	133	44.45	138	26.19
0.6	161	46.46	169	26.79
0.7	190	47.78	198	27.22
0.8	226	48.35	235	27.82
0.9	243	49.34	265	28.27

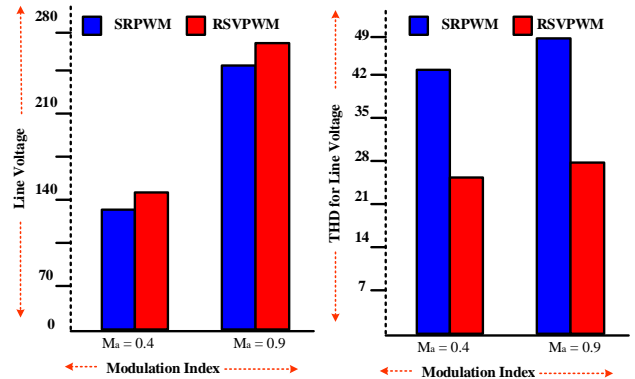


Fig.27. Line voltage and its THD for RSPWM and RSVPWM at 5 kHz

## 6. Conclusion

The conventional Random pulse width modulation (RPWM) method used in space vector pulse width modulation (SVPWM) inverter for spreading the harmonic noise cluster can excite the system resonant frequencies. The proposed method of this paper is randomized SVPWM technique for reducing acoustic noise in line voltage of two level

three phase VSI. Simulation and experimental results show that by using the proposed method, some unwanted noise can be reduced successfully. RSVPWM technique used for avoiding system resonant frequency excitation in squirrel cage induction motor for three phase VSI.

## References:

- [1] Marcel Dekker, Randall, Barron (2003), "Industrial noise control and acoustics", Louisiana Tech. University Ruston, Louisiana, ISBN: 0-8247-0701-X, USA.
- [2] M.Trzynadlowski, F.Blaabjerg, J.K.Pedersen, R.L.Kirlin, and S.Legowski (1994), "Random pulse width modulation technique for converter fed drive system- review", IEEE Trans. Ind. Appl., vol. 30, no. 5,1166-1175.
- [3] B.Jacob and M. Baiju (2011), "Spread spectrum modulation scheme for two level inverter using vector quantised space vector based pulse density modulation", IET Electr. Power Appl., vol.5, pp. 589-596.
- [4] Pedersen J K, Blaabjerg F and Frederiksen P (1993), "Reduction of acoustic noise emission in AC-machines by intelligent distributed random modulation", Proc. 5th Eur. Conf. Power Electron. Appl., pp. 369-375.
- [5] Blaabjerg F, Pedersen J.K, Ritchie E and Nielsen P (1995), "Determination of mechanical resonances in induction motors by random modulation and acoustic measurement", IEEE Trans. Ind. Appl., vol. 31, no. 4, pp. 823-829.
- [6] Bech M.M, Blaabjerg. F and Pedersen J. K. (2000), "Random modulation techniques with fixed switching frequency for three-phase power converters", IEEE Trans. Power Electron., vol. 15, no. 4, pp. 753-761.
- [7] Trzynadlowski A. M, Borisov K, Li Y, Qin L and Wang Z (2004), "Mitigation of electromagnetic interference and acoustic noise in vehicular drives by random pulse width modulation", Proc. Power Electron. Transp., pp. 67-71.
- [8] Borisov K, Calvert T.E, Kleppe J.A, Martin.M and Trzynadlowski.A.M. (2006), "Experimental investigation of a naval propulsion drive model with the PWM-based attenuation of the acoustic and electromagnetic noise", IEEE Trans. Ind. Electron., vol. 53, no. 2, pp. 450-457.
- [9] Schulz D and Kowalewski D. L. (2007), "Implementation of variable-delay random PWM for automotive applications", IEEE Trans. Veh. Technol., vol. 56, no. 3, pp. 1427-1433.
- [10] Qi C, Chen X and Qiu Y (2013), "Carrier-based randomized pulse position modulation of an indirect matrix converter for attenuating the harmonic peaks", IEEE Trans. Power Electron., vol. 28, no. 7, pp. 3539-3548.
- [11] Lai Y.-S, Chang Y.-T and Chen B.-Y (2013), "Novel random-switching PWM technique with the constant sampling frequency and constant inductor average current for digitally controlled converter", IEEE Trans. Ind. Electron., vol. 60, no. 8, pp. 3126-3135.
- [12] L.Mathe, P.R. Omand, J.K. Pedersen, "Shaping the spectra of the line to line voltage using signal injection in the common mode voltage", Industrial Electronics, 2009. IECON09, 35<sup>th</sup> Annual conference of IEEE, PP.1288-1293.
- [13] Oh S.-Y, Jung Y.-G., Yang S.-H. and Lim Y.-C. (2009), "Harmonic-spectrum spreading effects of two-phase random centred distribution PWM (DZRCD) scheme with dual zero vectors", IEEE Trans. Ind. Electron., vol. 56, no. 8, pp. 3013-3020.
- [14] Lai Y.-S and Chen B.-Y (2013), "New random PWM technique for a full-bridge DC/DC converter with harmonics intensity reduction and considering efficiency", IEEE Trans. Power Electron., vol. 28, no. 11, pp. 5013-5023.
- [15] Jiang D and Wang F (2013), "Variable switching frequency PWM for three-phase converters based on current ripple prediction", IEEE Trans. Power Electron., vol. 28, no. 11, pp. 4951-4961.
- [16] Mathe G, Lungeanu F, Sera D, Rasmussen P. O. and Pedersen J. K. (2012), "Spread spectrum modulation by using asymmetric-carrier random PWM", IEEE Trans. Ind. Electron., vol. 59, no. 10, pp. 3710-3718.
- [17] Máthé L (2010), "Product sound: Acoustically pleasant motor drives".
- [18] Peyghambari A, Dastfan A and Ahmadyfard A (2015), "Strategy for switching period selection in random pulse width modulation to shape the noise spectrum", IET Power Electron., vol. 8, pp. 517-523.
- [19] Kumar K. V, Michael P. A., John J. P. And Kumar D. S. S. (2010), "Simulation and comparison of SPWM and SVPWM control for three-phase inverter", ARPN J. Eng. Appl. Sci., vol. 5, pp. 61-74...
- [20] Bharatiraja, S.Jeevananthan,R.Lathe,"Vector Selection Approach-based Hexagonal Hysteresis Space Vector Current Controller for a Three-phase Diode Clamped MLI with Capacitor Voltage Balancing", IET Power Electronics,vol.9, Issue 7,pp.1350-1361,8 June 2016.
- [21] C. Bharatiraja, R. Latha, Dr. S. Jeevananthan, S. Raghu and Dr. S.S. Dash. "Design and Validation of Simple Space Vector PWM Scheme for Three-Level NPC - MLI with Investigation of Dc Link Imbalance using FPGA IP Core", Journal of Electrical Engineering, vol. 13, edition 1, pp 54-63, 2013.
- [22] C. Bharatiraja, S. Jeevananthan and JL munda "Timing Correction Algorithm for SVPWM Based Diode-Clamped MLI Operated in overmodulation Region", in IEEE journal of Selected topics in Power Electronics applications. vol. 6, no. 1, pp. 233-245, Mar. 2018.
- [23] M. Tariq, M. T. Iqbal, M. Meraj, A. Iqbal, A. I. Maswood, and C. Bharatiraja, "Design of a proportional resonant controller for packed U cell 5 level inverter for grid-connected applications," 2016 IEEE International Conference on Power Electronics, Drives and Energy Systems (PEDES), Trivendram, kerala, India. 14 -17 Dec 2016.
- [24] C. Bharatiraja, T. B. Prasad, and R. Latha, "Comparative realization of different SVPWM schemes in linear modulation using FPGA," 2008 IEEE Region 8 International Conference on Computational Technologies in Electrical and Electronics Engineering, Novosibirsk Scientific Centre, Novosibirsk, Russia.21-25 July 2008.